# Tumor suppressor Hippo/MST1 kinase mediates chemotaxis by regulating spreading and adhesion

Yulia Artemenko[a,1], Petros Batsios[b,1], Jane Borleis[a], Zachary Gagnon[a], Josephine Lee[a], Meino Rohlfs[b], Doriane Sanséau[a], Stacey S. Willard[a], Michael Schleicher[b], and Peter N. Devreotes[a,2]

[a]Department of Cell Biology, The Johns Hopkins University School of Medicine, Baltimore, MD 21205; and [b]Institute for Anatomy and Cell Biology, Ludwig Maximilian University, D-80336 Munich, Germany

Contributed by Peter N. Devreotes, July 4, 2012 (sent for review January 17, 2012)

**Chemotaxis depends on a network of parallel pathways that coordinate cytoskeletal events to bias cell movement along a chemoattractant gradient. Using a forward genetic screen in *Dictyostelium discoideum*, we identified the Ste20 kinase KrsB, a homolog of tumor suppressors Hippo and MST1/2, as a negative regulator of cell spreading and substrate attachment. The excessive adhesion of *krsB*$^-$ cells reduced directional movement and prolonged the streaming phase of multicellular aggregation. These phenotypes depended on an intact kinase domain and phosphorylation of a conserved threonine (T176) within the activation loop. Chemoattractants triggered a rapid, transient autophosphorylation of T176 in a heterotrimeric G protein-dependent and PI3K- and TorC2-independent manner. The active phosphorylated form of KrsB acts to decrease adhesion to the substrate. Taken together these studies suggest that cycling between active and inactive forms of KrsB may provide the dynamic regulation of cell adhesion needed for proper cell migration and chemotaxis. KrsB interacts genetically with another *D. discoideum* Hippo/MST homolog, KrsA, but the two genes are not functionally redundant. These studies show that Hippo/MST proteins, like the tumor suppressor PTEN and oncogenes Ras and PI3K, play a key role in cell morphological events in addition to their role in regulating cell growth.**

Directed migration along a chemical gradient, known as chemotaxis, is governed by a network of signaling events, many of which are conserved between the social amoeba *Dictyostelium discoideum* and human neutrophils. *D. discoideum* is a powerful model for chemotaxis and has been instrumental in elucidating the signaling events. Chemoattractant binding to G protein-coupled receptors leads to activation of several parallel pathways. One important module is the activation of PI3K with a concomitant reduction in PTEN levels at the leading edge of the cell (1, 2). The resulting enrichment of phosphatidylinositol-3,4,5-trisphosphate (PIP3) at the front of the cell recruits pleckstrin homology (PH) domain-containing proteins, including PKBA, CRAC, and PhdA (3–6). Another key event is activation of TorC2, which phosphorylates and activates AKT/PKBA as well as the *Dictyostelium*-specific myristoylated PKBR1 (7, 8). Chemoattractants also produce intracellular cGMP and activate the Rap1/Phg2 pathway, which together regulate myosin (9–11). Acting together, these signaling events bias actin polymerization and pseudopod extension in the direction of the gradient and organize the accumulation of myosin II away from the chemoattractant, allowing back contraction and consequent movement of the cell (12).

Interestingly, many of the key regulators of directed migration, such as Ras, PI3K, PTEN, and AKT, are most notable for their role in cell growth and survival. In *D. discoideum* these oncogenes and tumor suppressors instead act as positive or negative regulators, respectively, of cellular projections and thereby play a prominent role in cell migration (12). Another pathway that has been implicated in the regulation of cell growth and apoptosis involves Hippo. *Drosophila* Hippo and its mammalian homologs, mammalian Ste20-like kinase 1 (MST1, also known as "STK4") and MST2 (also known as "STK3"), have tumor-suppressor functions. Deletion of these genes leads to organ enlargement caused by increased cell growth and survival (13–20). Hippo and MST1/2 belong to the germinal center kinase II subfamily of the Ste20 family of kinases (21). Activation of these Ser/Thr kinases leads to a phosphorylation cascade that ultimately acts to inhibit the transcriptional coactivator Yorkie/YAP (22, 23).

Although their role in cell growth and survival is well established, it is unclear whether or in what capacity Hippo/MST Ste20 kinases function in chemotaxis. In one study of T cells, knock down of cellular levels of MST1 led to diminished integrin-mediated adhesion in response to chemokines or T-cell receptor ligation (24). In vivo, there was reduced thymocyte egress and lymphocyte accumulation at sites of inflammation (25, 26). However, earlier reports showed that active MST1 induces cell rounding and detachment, independently of caspase activation, in a variety of cell lines (27, 28). Thus these studies indicate that MST1 promotes integrin-mediated adhesion but negatively regulates cell spreading; considered together, these results are puzzling.

In a forward genetic screen for defects in chemotaxis in *D. discoideum*, we found a homolog of Hippo/MST1, kinase responsive to stress B (KrsB), to be an important regulator of multicellular development. This screen was based on the dependence of *D. discoideum* on chemotaxis throughout its life cycle. Under conditions of starvation, individual cells enter a developmental program in which they up-regulate a set of genes including cAR1, a receptor for the chemoattractant cAMP, necessary for chemotaxis and cell–cell communication (29). As cells begin secreting cAMP into their environment, surrounding amoebae chemotax toward this cue and secrete additional cAMP to attract more distal cells. "Streams" of cells aggregate into multicellular structures. The mutant with a disruption of KrsB was identified as a "streamer," meaning that its streaming aggregation stage persisted longer than that of WT cells. Subsequent studies showed that this mutant had an interesting defect in directed migration.

The phenotype of *D. discoideum* cells lacking KrsB function provided a unique opportunity to define the role of the Hippo/MST gene family in chemotaxis. In this study we assessed the behavior of cells lacking KrsB, KrsA, or both. We demonstrate that KrsB acts as a negative regulator of cell spreading and adhesion and that its loss interferes with chemotaxis. Furthermore, we show that chemoattractants stimulate a rapid, transient increase in activation-loop autophosphorylation of KrsB. We find that phosphorylation positively regulates KrsB function and speculate on the integration of these events during chemotaxis.

## Results

To study the function and regulation of KrsB, we generated cells lacking *krsB* by homologous recombination and confirmed successful gene disruption by Southern hybridization (Fig. S1 *A* and *B*). Immunoblotting with an antibody against the C-terminal part

Author contributions: Y.A., P.B., M.R., S.S.W., M.S., and P.N.D. designed research; Y.A., P.B., J.B., Z.G., J.L., M.R., D.S., and S.S.W. performed research; Y.A., P.B., and Z.G. contributed new reagents/analytic tools; Y.A., P.B., J.L., M.R., D.S., S.S.W., M.S., and P.N.D. analyzed data; and Y.A., M.S., and P.N.D. wrote the paper.

The authors declare no conflict of interest.

[1]Y.A. and P.B. contributed equally to this work.

[2]To whom correspondence should be addressed. E-mail: pnd@jhmi.edu.

This article contains supporting information online at www.pnas.org/lookup/suppl/doi:10.1073/pnas.1211304109/-/DCSupplemental.

of KrsB detected a band at the predicted size of 124 kDa that had almost uniform expression throughout development (Fig. S1*C*). The KrsB band was completely absent in *krsB*$^-$ cells (Fig. S1*D*).

To examine the role of KrsB in multicellular development, we assessed the phenotype of *krsB*$^-$ cells and *krsB*$^-$ cells expressing C-terminally GFP-tagged constructs of KrsB with various disrupted functional domains on bacterial lawns. This assay allows all the developmental stages to be observed in a plaque derived from a single cell. Compared with WT, plaques from two independent *krsB*$^-$ cell lines displayed an expanded region containing radial bands of cells or streams near the plaque perimeter (Fig. 1*A*). Because the two clones have very similar phenotypes, only the C1 clone is shown from now on. Full-length KrsB, as well as KrsB lacking the C-terminal regions homologous to domain III of Calpain ($KrsB_{\Delta C}$) reversed the streamer phenotype, whereas KrsB with a K52R mutation in the kinase domain ($KrsB_{K52R}$), or the $KrsB_{K52R/\Delta C}$ construct did not (Fig. 1 *B* and *C*). We also examined the behavior of *krsB*$^-$ cells on nonnutrient agar to assess the behavior of a synchronously starved population. *krsB*$^-$ cells showed a delay in the initiation of development, a prolonged streaming phase, and abnormal formation of multicellular structures (Fig. 1*D*). The aberrant timing of pattern formation of *krsB*$^-$ cells could not be attributed to a delayed expression of the developmental marker cAR1, which peaked at roughly the same time for WT and *krsB*$^-$ cells (Fig. S2*A*). WT cells formed normal fruiting bodies within 24 h, whereas even after 32 h those of *krsB*$^-$ cells were smaller and more numerous (Fig. 1*D*).

To confirm further that the morphological phenotype of *krsB*$^-$ cells is independent of developmental marker expression, we examined the aggregation of cells that had been synchronized with regular pulses of cAMP for 5 h. Under these conditions the expression of cAR1 reached the same maximal level in WT and *krsB*$^-$ cells ($n = 9$; $P > 0.05$ for WT vs. *krsB*$^-$ cells). The 5-h-stage WT cells polarized and formed well-defined streams by 1 h after plating. These streams coalesced rapidly into aggregates by 2 h (Fig. 1*E*). *krsB*$^-$ cells similarly polarized and formed streams by 1 h after plating; however, these streams persisted beyond 3 h after plating. These data confirm that KrsB is required for the formation of the proper multicellular pattern in similarly differentiated cells.

We further examined whether KrsB is required for other aspects of development. Following aggregation, *D. discoideum* cells form a multicellular organism that undergoes several morphological changes, including slug formation. Slugs exhibit the ability to migrate directionally toward light, a process known as "phototaxis," which is dependent on the migratory properties of the individual cells within the slug. Unlike WT, *krsB*$^-$ slugs completely failed to migrate toward a light source, and this defect was rescued by expression of full-length KrsB tagged with GFP at the N terminus (Fig. S2*B*).

To examine the role of KrsB during directed migration in a gradient, we subjected aggregation-competent *krsB*$^-$ and WT cells plated in a chambered coverglass to a micropipette releasing cAMP (Fig. 2 *A* and *B*; Table S1; and Movies S1 and S2). Under these conditions WT cells migrated robustly toward the chemoattractant source. *krsB*$^-$cells also were able to sense the gradient and eventually migrate toward the micropipette; however, in contrast to WT cells, they often appeared to be stuck to the surface and displayed aberrant movement toward the micropipette. Consequently, *krsB*$^-$ cells showed a significant reduction in directional persistence ($44.1 \pm 0.7\%$; $P < 0.01$), chemotactic speed ($56 \pm 8\%$; $P < 0.05$), and chemotactic index ($61 \pm 5\%$; $P < 0.05$) compared with WT (mean ± SE; $n = 3$). To confirm that the absence of KrsB is responsible for the defects observed in *krsB*$^-$ cells, we performed a micropipette assay on *krsB*$^-$ cells expressing C-terminally GFP-tagged full-length KrsB, $KrsB_{\Delta C}$, or empty vector (Fig. 2*C* and Movies S3 and S4). Both KrsB constructs were able to improve the chemotaxis of *krsB*$^-$ cells.

We also examined chemotaxis in a small population assay (Fig. S2 *C* and *D* and Table S1). In this assay, which is performed on a hydrophobic agar surface, the defect caused by the absence of KrsB was less pronounced than in a micropipette assay. Only motility speed was reduced significantly, by $22 \pm 6\%$ for *krsB*$^-$ compared with WT cells (mean ± SE; $n = 6$; $P < 0.05$). The observed defect may be less pronounced in this assay than in the micropipette assay because of the differences in the surfaces (see below).

To determine whether defective chemotaxis in the absence of KrsB is caused by inappropriate activation of known regulators of directed motility, we tested Ras activation, PIP3 production, and actin polymerization in a gradient and in response to global stimulation with cAMP. In a micropipette assay both PIP3

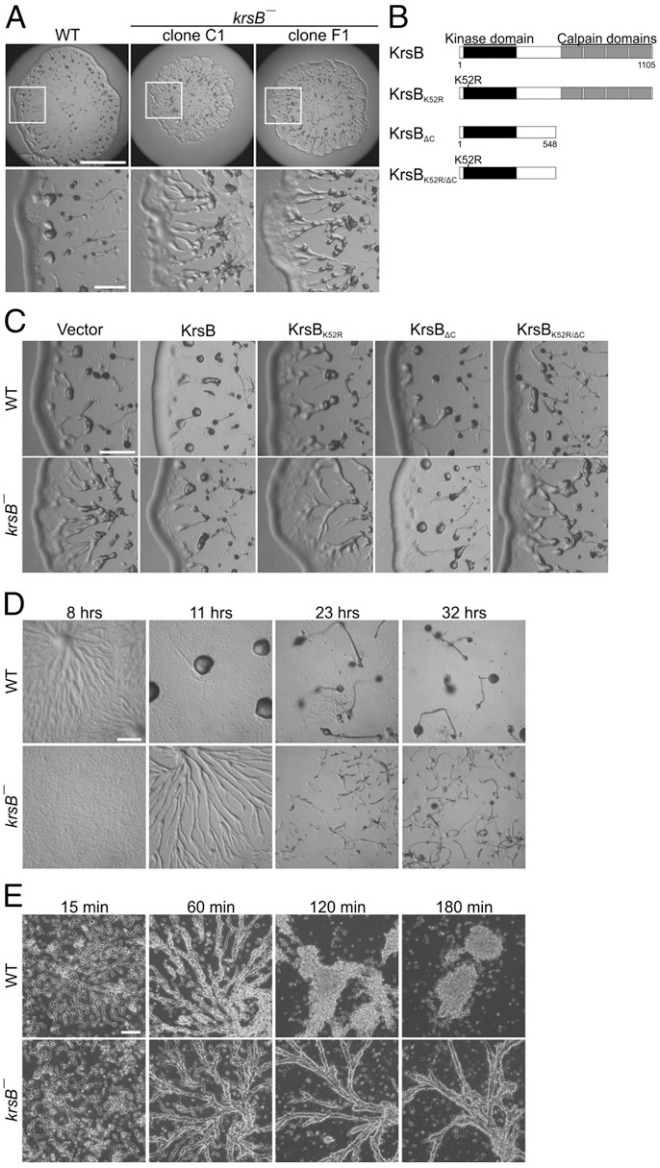


**Fig. 1.** KrsB is required for proper morphological development and multicellular behavior. (*A*) (*Upper*) WT and two independent *krsB*$^-$ cell lines were plated on a *Klebsiella aerogenes* lawn, and plaques were imaged after 4 d. (Scale bar: 5 mm.) (*Lower*) High-magnification views of plaque edges. (Scale bar: 1 mm.) (*B*) Schematic of the expression constructs used in this study. (*C*) WT (*Upper*) and *krsB*$^-$ (*Lower*) cells expressing C-terminally GFP-tagged KrsB constructs or empty vector were treated as in *A*. (Scale bar: 1 mm.) (*D*) Cells were plated on nonnutrient agar and imaged at the indicated time points. (Scale bar: 0.5 mm.) (*E*) Aggregation-competent cells were plated under buffer and imaged at the indicated time points. (Scale bar: 100 μm.)

CELL BIOLOGY

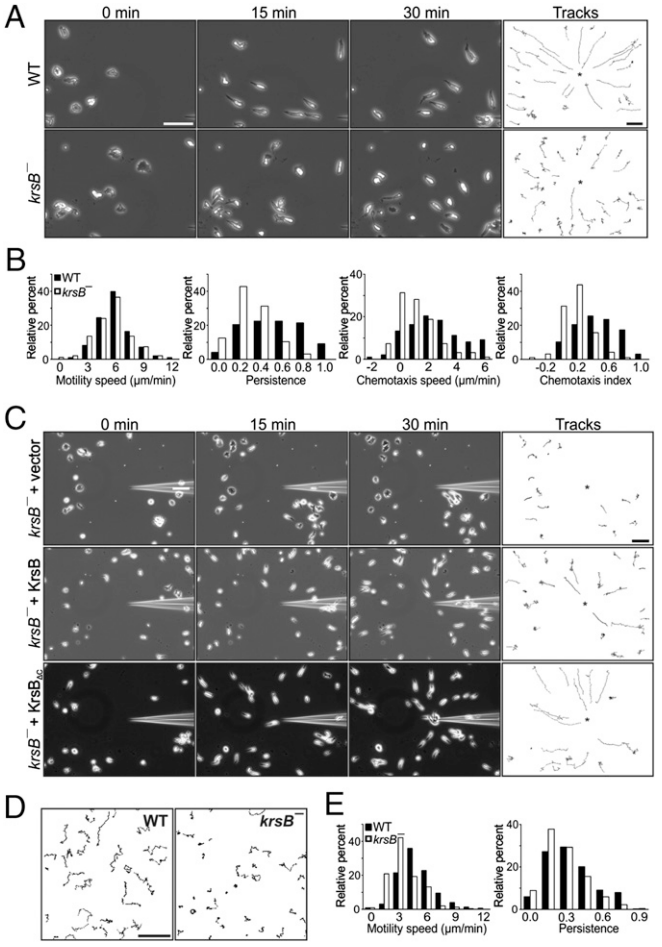


**Fig. 2.** KrsB is required for properly directed migration and random motility. (*A* and B) Aggregation-competent WT and *krsB*$^-$ cells plated on a chambered coverglass were exposed to a micropipette filled with 10 μM cAMP and were imaged every 30 s for 30 min. (*A*) Tracks of individual cells over the 30-min period, as well as snapshots (of the top left quadrant only) taken at the indicated time points are shown. (Scale bar: 50 μm.) (*B*) Behavior of 98 WT and 96 *krsB*$^-$ cells obtained from three independent experiments was analyzed for various chemotaxis parameters. (*C*) Aggregation-competent *krsB*$^-$ cells expressing empty vector or C-terminally GFP-tagged KrsB or KrsB$_{\Delta C}$ were treated as in *A*. (Scale bar: 50 μm.) (*D* and *E*) Vegetative WT and *krsB*$^-$ cells were plated on a chambered coverglass in growth medium. (*D*) Cells were imaged every 30 s for 30 min. Tracks of individual cells over the 30-min period are shown. (Scale bar: 100 μm.) (*E*) Behavior of 452 WT and 560 *krsB*$^-$ cells obtained from three independent experiments was analyzed for motility, speed, and persistence.

production and actin polymerization, assessed by recruitment of the PH domain from CRAC or LimE$_{\Delta coil}$, respectively, did not appear different in migrating *krsB*$^-$ and WT cells (Fig. S3 *A* and *B*). Similarly, following global stimulation with cAMP, the Ras-binding domain of Raf, used as a reporter for Ras activation, as well as PH$_{CRAC}$ and LimE$_{\Delta coil}$, showed transient translocation to the plasma membrane in both cell lines (Fig. S3*C*). Thus, the localization of leading-edge markers does not appear to be substantially different in WT and *krsB*$^-$ cells.

We next assessed whether *krsB*$^-$ cells have reduced chemotaxis specifically to cAMP or instead have a general defect in directed migration. We examined the random motility of vegetative WT and *krsB*$^-$ cells in growth medium (Fig. 2 *D* and *E* and Table S1). Motility speed was reduced significantly, by 29 ± 5%, for *krsB*$^-$ cells compared with WT (mean ± SE; $n = 3$; $P < 0.05$). Furthermore, migration of vegetative *krsB*$^-$ cells exposed to a gradient of folic acid also was impaired compared with WT cells (Fig. S2*E*).

Because *krsB*$^-$ cells often appeared stuck during their migration, we examined the attachment of these cells to the substrate in more detail. Under phase-contrast microscopy vegetative *krsB*$^-$ cells appeared more adhered and flattened than WT cells (Fig. 3*A*). We quantified the surface area-to-volume ratio for WT and *krsB*$^-$ cells that express cAR1 uniformly across the plasma membrane (Fig. 3*B*). In this assay, the surface area-to-volume ratio was 0.09 ± 0.04 μm$^{-1}$ for WT cells and increased to 0.15 ± 0.03 μm$^{-1}$ for *krsB*$^-$ cells (mean ± SD; $n = 12$ for WT, $n = 20$ for *krsB*$^-$ cells; $P < 0.001$). This difference was not caused by a change in the total volume of the cells ($P > 0.05$) (Fig. S4*A*). In agreement with these data, the area in contact with the surface measured by interference reflection microscopy (IRM) was increased significantly for *krsB*$^-$ as compared with WT cells. The mean contact surface was 62 ± 3 μm$^2$ for WT (mean ± SE, $n = 402$), 82 ± 5 μm$^2$ for *krsB*$^-$ clone C1 (mean ± SE, $n = 328$; $P < 0.01$ vs. WT), and 104 ± 5 μm$^2$ for *krsB*$^-$ clone F1 (mean ± SE, $n = 317$; $P < 0.001$).

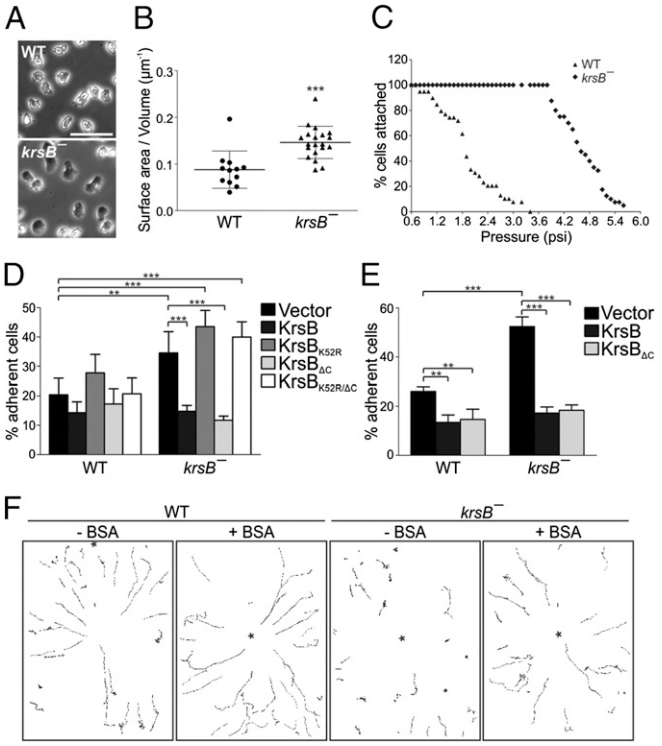


**Fig. 3.** Increased spreading and adhesion of *krsB*$^-$ cells is responsible, in part, for their defective chemotaxis. Analysis was performed on WT and *krsB*$^-$ cells. (*A*) Phase-contrast images of vegetative cells in glass-bottomed chambers in growth medium. (Scale bar: 50 μm.) (*B*) Vegetative cells expressing cAR1-mCherry were plated in glass-bottomed chambers in phosphate buffer, and serial sections were imaged with a spinning disk confocal microscope. The area of each slice from 12 WT and 20 *krsB*$^-$ cells was measured to derive the surface area-to-volume ratio. Data are shown as mean ± SD; ***$P < 0.001$. (*C*) Vegetative cells were loaded into a microfluidic device, exposed to constant flow with pressure increasing by 0.1 psi every 2 min, and imaged every 30 s. The percentage of cells remaining attached to the surface was calculated before each pressure increase. (*D* and *E*) Vegetative cells expressing either empty vector or the indicated C-terminally GFP-tagged KrsB constructs were subjected to a rotational adhesion assay at 150 rpm (*D*) or 100 rpm (*E*). Data derived from four (*D*) or three (*E*) separate experiments, each performed in duplicate, are shown as mean ± SE; **$P < 0.01$; ***$P < 0.001$. (*F*) Aggregation-competent cells plated in glass-bottomed chambers with or without 0.2% BSA coating were exposed to a micropipette filled with 10 μM cAMP and were imaged every 15 s for 20 min. Tracks of individual cells over the 20-min period are shown. (Scale bar: 100 μm.)

To determine whether the increased contact area of *krsB*$^-$ cells confers stronger adhesion, we subjected cells to sheer flow. First, cells in a microfluidic device were exposed to 0.1-psi increments in pressure every 2 min (Fig. 3*C* and Movies S5 and S6). Under these conditions all WT cells detached by 3.4 psi, but *krsB*$^-$ cells did not begin to detach until ~3.9 psi and did not detach completely until 5.6 psi. In a second assay cells were plated on tissue-culture dishes and rotated at a constant speed, and floating and adherent cells were enumerated to calculate the relative percentage of adherent cells. Under standard conditions, when plates were rotated at 150 rpm for 1 h, *krsB*$^-$ cells had an 82 ± 19% increase in adhesion vs. WT cells (mean ± SE; $n = 4$; $P < 0.01$) (Fig. 3*D*). This increase was reversed by expressing C-terminally GFP-tagged full-length KrsB or $KrsB_{\Delta C}$ but not $KrsB_{K52R}$ or $KrsB_{K52R/\Delta C}$. Because expression of KrsB appeared to reduce adhesion of WT cells slightly, we performed the assay at a reduced speed of 100 rpm to amplify the differences (Fig. 3*E*). Indeed, under these conditions, both KrsB and $KrsB_{\Delta C}$ significantly reduced WT adhesion, by 49 ± 8% and 46 ± 12%, respectively (mean ± SE; $n = 3$; $P < 0.01$). Together, these data establish that KrsB is a negative regulator of adhesion, and this function depends on its intact kinase domain.

Because absence of KrsB leads to a robust enhancement of cell adhesion to the substrate, we examined whether this enhanced adhesion is the reason for defective chemotaxis of *krsB*$^-$ cells. To test this possibility, we performed the micropipette assay on a glass surface precoated with BSA to render it more slippery (Fig. 3*F*, Fig. S4*B*, and Table S2). WT cells showed an increase in chemotaxis speed and persistence under these conditions (3.2 ± 0.8- and 1.6 ± 0.1-fold, respectively; mean ± SE; $n = 3$; $P < 0.05$). However, the improvement was much more pronounced for *krsB*$^-$ cells with a 14 ± 8-fold increase in chemotaxis speed (mean ± SE; $n = 3$; $P < 0.05$) and a 2.6 ± 0.5-fold increase in directional persistence (mean ± SE; $n = 3$; $P < 0.01$). Importantly, *krsB*$^-$ cells showed a significant improvement in the chemotaxis index, by 5.2 ± 1.5-fold, for the BSA-coated as compared with uncoated surface (mean ± SE; $n = 3$; $P < 0.05$).

In vitro kinase activity of MST1 depends on the phosphorylation of Thr183 in the activation loop (28), so we tested whether KrsB also is regulated by phosphorylation. The sequence surrounding Thr183 (Thr176 in *D. discoideum* KrsB) is conserved completely between human MST1 and *D. discoideum* KrsB sequences (Fig. 4*A*). To test whether Thr176 in KrsB is phosphorylated, we probed lysates from vegetative WT and *krsB*$^-$ cells expressing various KrsB constructs with an antibody that specifically recognizes phosphorylated Thr183 of MST1 (Fig. 4*B*). C-terminally GFP-tagged full-length KrsB and $KrsB_{\Delta C}$ indeed were phosphorylated in both WT and *krsB*$^-$ cells. The intact kinase domain of KrsB appeared to be essential for this phosphorylation, because GFP-tagged $KrsB_{K52R}$ and $KrsB_{K52R/\Delta C}$ were not phosphorylated. Expression of GFP-tagged KrsB or $KrsB_{\Delta C}$ also led to phosphorylation of endogenous KrsB in WT cells that was not seen for $KrsB_{K52R}$ or $KrsB_{K52R/\Delta C}$ cells. This result suggests that phosphorylation of KrsB at Thr176 is likely to be mediated by autophosphorylation by other KrsB molecules. To demonstrate autophosphorylation directly, we immunoprecipitated various C-terminally GFP-tagged KrsB constructs and performed an in vitro kinase assay in the presence of [$\gamma$-$^{32}$P]ATP (Fig. 4*C*). Only full-length KrsB and $KrsB_{\Delta C}$ showed a distinct radiolabeled band. We further assessed the ability of KrsB molecules to carry out intermolecular phosphorylation. We performed the kinase assay on $KrsB_{K52R}$, $KrsB_{\Delta C}$, or a mixture of the two (Fig. 4*D*). Although $KrsB_{K52R}$ alone did not show any autophosphorylation, this construct became phosphorylated in the presence of $KrsB_{\Delta C}$.

To determine whether Thr176 phosphorylation is regulated by chemoattractants, we globally stimulated aggregation-competent WT cells with cAMP and checked for KrsB phosphorylation at several time points (Fig. 4*E*). cAMP stimulated a transient increase in KrsB phosphorylation. At 9 °C, peak phosphorylation was observed at 30 s poststimulation, with a 1.9 ± 0.5-fold

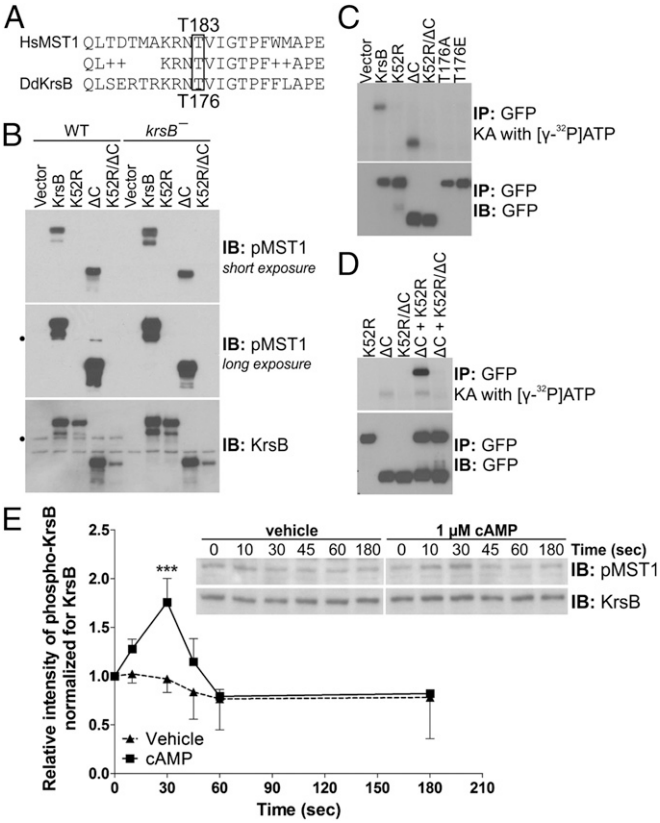


**Fig. 4.** Activation loop phosphorylation of KrsB is regulated by cAMP. (*A*) Alignment of human MST1 and *D. discoideum* KrsB protein sequence surrounding Thr183 in hMST1. (*B*) Vegetative WT and *krsB*$^-$ cells expressing C-terminally GFP-tagged KrsB constructs or empty vector were lysed and immunoblotted (IB) with an antibody against MST1 phosphorylated on Thr183 (pMST1) or KrsB. The black circle indicates the position of the endogenous KrsB band. (*C* and *D*) C-terminally GFP-tagged KrsB constructs expressed in *krsB*$^-$ cells were immunoprecipitated (IP) with antibodies against GFP and subjected to an in vitro kinase assay (KA) in the presence of [$\gamma$-$^{32}$P]ATP either alone (*C*) or in various combinations (*D*). Immunoprecipitates also were immunoblotted with an antibody against GFP. (*E*) Aggregation-competent WT cells were treated with 1 μM cAMP or vehicle, lysed at the indicated times, and immunoblotted as in *B*. Densitometric data for phospho-MST1 normalized for the KrsB signal were obtained from four separate experiments and are expressed as mean ± SD. ***$P < 0.001$.

increase compared with treatment with vehicle alone (mean ± SE; $n = 4$; $P < 0.001$). Phosphorylation was dependent on heterotrimeric G proteins, as shown by the lack of cAMP-stimulated KrsB phosphorylation in *g$\beta^-$* cells (Fig. S5*A*). To test if KrsB phosphorylation is mediated via known pathways important for chemotaxis, we treated cells with 100 μM LY294002, a concentration that inhibits both PI3K and TorC2 (Fig. S5*B*) (30). cAMP-stimulated KrsB phosphorylation was not affected by LY294002 pretreatment and thus is independent of these pathways. In contrast to the endogenous KrsB, the GFP-tagged form was constitutively phosphorylated even when it was expressed below endogenous levels (Fig. S5*C*).

To assess whether Thr176 phosphorylation is required for KrsB function, we examined the ability of GFP-tagged KrsB constructs with T176A and T176E substitutions to rescue *krsB*$^-$ phenotypes. As expected, neither of the Thr176 substitutions was recognized by the antibody against phosphorylated Thr183 in MST1 (Fig. 5*A*). On nonnutrient agar, $KrsB_{T176A}$ failed to rescue the prolonged streaming and the abnormal fruiting body morphology of *krsB*$^-$ cells (Fig. 5*B*). On the other hand, $KrsB_{T176E}$ appeared to reverse the *krsB*$^-$ phenotype partially, although it was not as effective as WT KrsB. Similarly, in an adhesion assay,

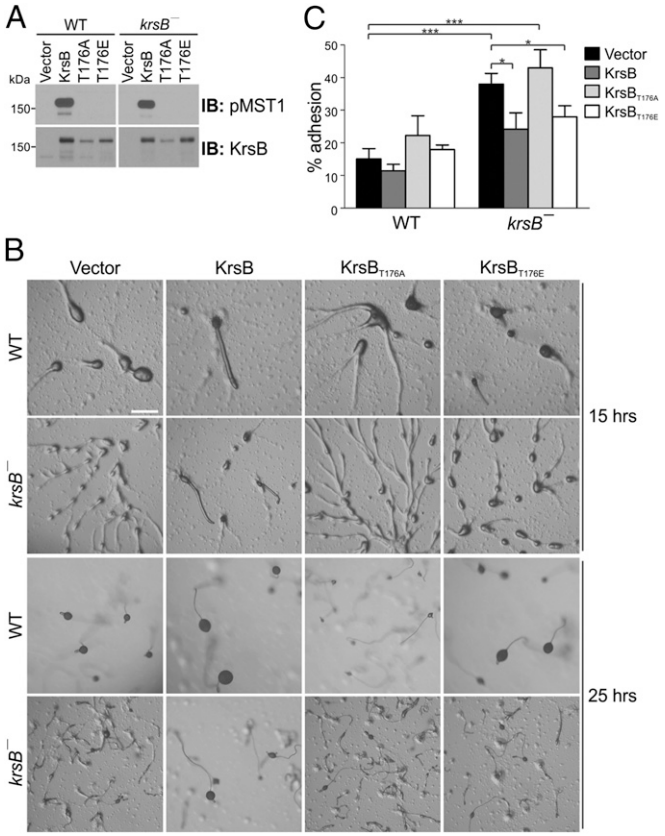


**Fig. 5.** Activation loop phosphorylation is required for KrsB function. Analysis was performed on WT and *krsB*$^-$ cells expressing empty vector or C-terminally GFP-tagged KrsB constructs under the control of a doxycycline-inducible promoter. (*A*) Vegetative cells were lysed and immunoblotted with an antibody against MST1 phosphorylated on Thr183 (pMST1) or KrsB. (*B*) Cells were plated on nonnutrient agar and were imaged at the indicated time points. (Scale bar: 0.5 mm.) (*C*) Vegetative cells were subjected to a rotational adhesion assay at 150 rpm. Data derived from three separate experiments, each performed in duplicate, are shown as mean ± SE. **P* < 0.05; ****P* < 0.001.

KrsB$_{T176A}$ failed to reverse the increased adhesion of *krsB*$^-$ cells ($n = 3$; $P > 0.05$) (Fig. 5*C*). Conversely, both WT KrsB and KrsB$_{T176E}$ significantly decreased adhesion of *krsB*$^-$ cells, by 36 ± 10% and 25 ± 12%, respectively (mean ± SE; $n = 3$; $P < 0.05$). Thus, phosphorylation of Thr176 is essential for KrsB function in multicellular development and adhesion, and optimal function might require regulation of the phosphorylation.

To address whether KrsB is functionally redundant with its *D. discoideum* homolog KrsA, we overexpressed KrsA in *krsB*$^-$ cells to test its ability to rescue the streamer phenotype and also disrupted both *krsA* and *krsB* genes in the same cells. Expression of KrsA tagged with GFP on the N terminus failed to rescue the streaming phenotype of *krsB*$^-$ cells on a bacterial lawn (Fig. S6*A*). Thus, excess KrsA cannot compensate for lack of KrsB during multicellular development. After deleting both the *krsA* and *krsB* genes, we confirmed the absence of the respective protein products using antibodies that detect endogenous KrsA and KrsB (Fig. S1*D*). Consistent with published findings (31, 32), we observed only subtle changes of phenotype for *krsA*$^-$ cells alone; however, disruption of *krsA* modified the phenotype of *krsB*$^-$ cells (Fig. S6 *B* and *C*). Overall plaque morphology for *krsA*/*B*$^-$ cells on a bacterial lawn appeared similar to *krsB*$^-$ cells, except there was no expanded region of streaming cells (Fig. S6*B*). On nonnutrient agar, *krsA*/*B*$^-$ cells had a delay in the initiation of development similar to that in *krsB*$^-$ cells (Fig. S6*C*). However, the streams seemed to break up earlier in the *krsA*/*B*$^-$ cells than in *krsB*$^-$ cells. Although the final fruiting morphology in *krsA*/*B*$^-$ cells resembled the *krsB*$^-$ cell phenotype at 24 h, by 48 h *krsA*/*B*$^-$ cells seemed to catch up to WT cells, but *krsB*$^-$ cells retained the small fruiting body morphology.

## Discussion

Fig. 6 summarizes our characterization of the Hippo/MST homolog KrsB identified in a nonbiased screen for chemotaxis mutants. KrsB undergoes reversible intermolecular autophosphorylation regulated by chemoattractant in a heterotrimeric G protein-dependent and PI3K- and TorC2-independent manner. The phospho-mimetic form of KrsB or the expressed WT version of KrsB, which is constitutively phosphorylated (Fig. S5*C*), makes cells less adhesive (Fig. 3*E*), whereas cells containing no KrsB or the nonphosphorylatable form are more adhesive. The increased cell spreading and adhesion of *krsB*$^-$ cells causes aberrant motility and chemotaxis, which lead to a characteristic streamer phenotype.

Reversible KrsB phosphorylation is important for the dynamic regulation of cell adhesion, which is required for proper cell migration and chemotaxis. During the migration cycle, attachment to the substrate must be regulated temporally and spatially. The timing of cAMP-stimulated KrsB phosphorylation is similar to the timing of the activation and recruitment of many leading-edge markers in a migrating cell, suggesting that KrsB activation might occur at the front of a cell. We have not observed GFP-tagged KrsB, which is constitutively activated, at the front edge of the cell. However, we found previously that TorC2 can phosphorylate its substrates PKBA and PKBR1 only at the leading edge of the cell, even though its subunits appear to be cytosolic (8). If KrsB indeed is activated at the leading edge, it raises the question of why a negative regulator of adhesion would be needed at the front of a cell.

A role for Hippo/MST homologs in adhesion is not confined to *D. discoideum*. Our observations that KrsB is a negative regulator of cell adhesion are consistent with the cell rounding and detachment observed with active MST1 overexpression in NIH 3T3 (28) and HeLa cells (27). However, they are in contrast to the findings of Katagiri et al. (24) that knock down of MST1 leads to reduced adhesion of T lymphocytes in response to chemokine stimulation. However, the adhesion examined in the lymphocyte study was exclusively integrin dependent and consequently might involve a mechanism different from the nonintegrin-based adhesion of *D. discoideum* cells (33, 34). Interestingly, accumulating evidence suggests that neutrophils can migrate in an integrin-independent fashion in various environments, including on fibrin matrices (35) and soft hydrogels (36). *D. discoideum* offers unique

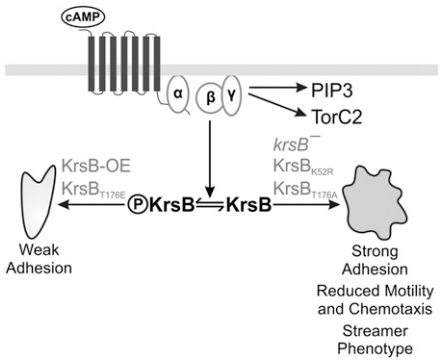


**Fig. 6.** Proposed model for KrsB function. Chemoattractants trigger transient activation of KrsB by intermolecular autophosphorylation in a heterotrimeric G protein-dependent and PI3K- and TorC2-independent manner. Expression of the phospho-mimetic form (T176E) or WT KrsB, which is constitutively phosphorylated, leads to reduced adhesion. On the other hand, *krsB*$^-$ cells and cells in which KrsB is inactive (KrsB$_{T176A}$ or KrsB$_{K52R}$) have increased adhesion that causes reduced motility and chemotaxis, resulting in a streamer phenotype.

advantages as a model for understanding the mechanisms of integrin-independent adhesion and migration.

By two different measures *krsB*$^-$ cells are more spread than WT cells. The enhanced spreading of a cell can be brought about by reducing cortical tension or increasing the contact area. The increased adhesion of *krsB*$^-$ cells is proportional to the enhanced spreading of these cells and is not likely to be caused by stronger adhesion per unit area, although the latter was not measured in this study. When *krsB*$^-$cells are put on a slippery surface, cell morphology is restored toward WT levels, suggesting that the increased adhesiveness, and not reduced cortical tension, is responsible for the greater contact area of these cells.

Extensive analysis of chemotaxis in *D. discoideum* previously has not uncovered any of the downstream components of the canonical Hippo/MST pathway. Typically, the Hippo/MST cascade regulates transcriptional events that control cell growth. We cannot rule out the possibility that KrsB regulates transcription, although we observe that rescue of the *krsB*$^-$ phenotype closely parallels the time course of the induction of KrsB expression. More likely, KrsB directly controls cell adhesion and morphology. Further studies are needed to position KrsB within the signaling network. We have shown that KrsB activation is mediated by G protein-coupled receptors and is independent of the key regulators TorC2 and PI3K. It is possible that KrsB participates in the Rap1/Phg2 pathway, which has been suggested to modulate both adhesion and chemotaxis by promoting myosin II disassembly at the leading edge of the cell (10, 11).

Typically, chemoattractants exert their effects on the cytoskeleton within seconds. Like chemoattractants, growth factors trigger rapid cytoskeletal events when first added to a cell, but their effects on growth require sustained application. Our characterization of KrsB adds to the list of signaling molecules, such as components of the Ras and PI3K pathways, which regulate growth as well as motility and chemotaxis. The direction of the regulation of motility and chemotaxis also is correlated with the effects on growth, so that oncogenes generally promote cell spreading, whereas tumor suppressors inhibit spreading. Our characterization of KrsB is consistent with this theme, because Hippo/MST homologs are tumor suppressors, and the loss of KrsB leads to excessive spreading.

## Materials and Methods

KrsB and krsA gene disruptions and GFP-tagged KrsB or KrsA expression were performed in the Ax2 strain of *D. discoideum* cells according to standard procedures. Aggregation-competent cells were obtained by 5 h starvation with the addition of 50 nM cAMP every 6 min for the last 4 h. Detailed descriptions of the materials and methods are provided in *SI Materials and Methods*.

**ACKNOWLEDGMENTS.** We thank Dr. R. R. Kay for providing the restriction enzyme-mediated integration mutant collection used in the screen in which KrsB was identified; Drs. S. Das, C. P. McCann, and C. A. Parent for assistance with interference reflection microscopy imaging; Drs. P. Iglesias and Y. Xiong for the video analysis software; Dr. P. J. van Haastert for the doxycycline-inducible expression vector and the $RBD_{Raf}$-GFP construct; Dr. C. A. Parent for the $PH_{CRAC}$-GFP plasmid; Dr. D. N. Robinson for the GFP-$LimE_{\Delta coil}$ plasmid; Drs. K. F. Swaney and H. Cai from the P.N.D. laboratory for the pKF3 expression vector and the cAR1-mCherry construct, respectively; and P. Vaswani for help with cloning the GFP-tagged KrsB constructs. We also thank the staff at the dictyBase database for annotation of the *krsB* gene. This work was supported by National Institutes of Health Grants GM34933 and GM28007 (to P.N.D.) and Deutsche Forschungsgemeinschaft Grants SFB914-A7 and Schl 204/10 (to M.S.).

1. Funamoto S, Meili R, Lee S, Parry L, Firtel RA (2002) Spatial and temporal regulation of 3-phosphoinositides by PI 3-kinase and PTEN mediates chemotaxis. *Cell* 109:611–623.
2. Iijima M, Devreotes PN (2002) Tumor suppressor PTEN mediates sensing of chemoattractant gradients. *Cell* 109:599–610.
3. Huang YE, et al. (2003) Receptor-mediated regulation of PI3Ks confines PI(3,4,5)P3 to the leading edge of chemotaxing cells. *Mol Biol Cell* 14:1913–1922.
4. Parent CA, Blacklock BJ, Froehlich WM, Murphy DB, Devreotes PN (1998) G protein signaling events are activated at the leading edge of chemotactic cells. *Cell* 95:81–91.
5. Meili R, et al. (1999) Chemoattractant-mediated transient activation and membrane localization of Akt/PKB is required for efficient chemotaxis to cAMP in Dictyostelium. *EMBO J* 18:2092–2105.
6. Funamoto S, Milan K, Meili R, Firtel RA (2001) Role of phosphatidylinositol 3′ kinase and a downstream pleckstrin homology domain-containing protein in controlling chemotaxis in dictyostelium. *J Cell Biol* 153:795–810.
7. Lee S, et al. (2005) TOR complex 2 integrates cell movement during chemotaxis and signal relay in Dictyostelium. *Mol Biol Cell* 16:4572–4583.
8. Kamimura Y, et al. (2008) PIP3-independent activation of TorC2 and PKB at the cell's leading edge mediates chemotaxis. *Curr Biol* 18:1034–1043.
9. Bosgraaf L, et al. (2002) A novel cGMP signalling pathway mediating myosin phosphorylation and chemotaxis in Dictyostelium. *EMBO J* 21:4560–4570.
10. Gebbie L, et al. (2004) Phg2, a kinase involved in adhesion and focal site modeling in Dictyostelium. *Mol Biol Cell* 15:3915–3925.
11. Jeon TJ, Lee D-J, Merlot S, Weeks G, Firtel RA (2007) Rap1 controls cell adhesion and cell motility through the regulation of myosin II. *J Cell Biol* 176:1021–1033.
12. Swaney KF, Huang CH, Devreotes PN (2010) Eukaryotic chemotaxis: A network of signaling pathways controls motility, directional sensing, and polarity. *Annu Rev Biophys* 39:265–289.
13. Wu S, Huang J, Dong J, Pan D (2003) hippo encodes a Ste-20 family protein kinase that restricts cell proliferation and promotes apoptosis in conjunction with salvador and warts. *Cell* 114:445–456.
14. Udan RS, Kango-Singh M, Nolo R, Tao C, Halder G (2003) Hippo promotes proliferation arrest and apoptosis in the Salvador/Warts pathway. *Nat Cell Biol* 5: 914–920.
15. Harvey KF, Pfleger CM, Hariharan IK (2003) The Drosophila Mst ortholog, hippo, restricts growth and cell proliferation and promotes apoptosis. *Cell* 114:457–467.
16. Jia J, Zhang W, Wang B, Trinko R, Jiang J (2003) The Drosophila Ste20 family kinase dMST functions as a tumor suppressor by restricting cell proliferation and promoting apoptosis. *Genes Dev* 17:2514–2519.
17. Pantalacci S, Tapon N, Léopold P (2003) The Salvador partner Hippo promotes apoptosis and cell-cycle exit in Drosophila. *Nat Cell Biol* 5:921–927.
18. Zhou D, et al. (2009) Mst1 and Mst2 maintain hepatocyte quiescence and suppress hepatocellular carcinoma development through inactivation of the Yap1 oncogene. *Cancer Cell* 16:425–438.
19. Lu L, et al. (2010) Hippo signaling is a potent in vivo growth and tumor suppressor pathway in the mammalian liver. *Proc Natl Acad Sci USA* 107:1437–1442.
20. Song H, et al. (2010) Mammalian Mst1 and Mst2 kinases play essential roles in organ size control and tumor suppression. *Proc Natl Acad Sci USA* 107:1431–1436.
21. Dan I, Watanabe NM, Kusumi A (2001) The Ste20 group kinases as regulators of MAP kinase cascades. *Trends Cell Biol* 11:220–230.
22. Huang J, Wu S, Barrera J, Matthews K, Pan D (2005) The Hippo signaling pathway coordinately regulates cell proliferation and apoptosis by inactivating Yorkie, the Drosophila Homolog of YAP. *Cell* 122:421–434.
23. Dong J, et al. (2007) Elucidation of a universal size-control mechanism in Drosophila and mammals. *Cell* 130:1120–1133.
24. Katagiri K, Imamura M, Kinashi T (2006) Spatiotemporal regulation of the kinase Mst1 by binding protein RAPL is critical for lymphocyte polarity and adhesion. *Nat Immunol* 7:919–928.
25. Dong Y, et al. (2009) A cell-intrinsic role for Mst1 in regulating thymocyte egress. *J Immunol* 183:3865–3872.
26. Katagiri K, et al. (2009) Mst1 controls lymphocyte trafficking and interstitial motility within lymph nodes. *EMBO J* 28:1319–1331.
27. Lee K-K, Ohyama T, Yajima N, Tsubuki S, Yonehara S (2001) MST, a physiological caspase substrate, highly sensitizes apoptosis both upstream and downstream of caspase activation. *J Biol Chem* 276:19276–19285.
28. Glantschnig H, Rodan GA, Reszka AA (2002) Mapping of MST1 kinase sites of phosphorylation. Activation and autophosphorylation. *J Biol Chem* 277:42987–42996.
29. Parent CA, Devreotes PN (1996) Molecular genetics of signal transduction in Dictyostelium. *Annu Rev Biochem* 65:411–440.
30. Kortholt A, et al. (2011) Dictyostelium chemotaxis: Essential Ras activation and accessory signalling pathways for amplification. *EMBO Rep* 12:1273–1279.
31. Arasada R, et al. (2006) Characterization of the Ste20-like kinase Krs1 of Dictyostelium discoideum. *Eur J Cell Biol* 85:1059–1068.
32. Muramoto T, Kuwayama H, Kobayashi K, Urushihara H (2007) A stress response kinase, KrsA, controls cAMP relay during the early development of Dictyostelium discoideum. *Dev Biol* 305:77–89.
33. Fey P, Stephens S, Titus MA, Chisholm RL (2002) SadA, a novel adhesion receptor in Dictyostelium. *J Cell Biol* 159:1109–1119.
34. Cornillon S, et al. (2006) An adhesion molecule in free-living Dictyostelium amoebae with integrin beta features. *EMBO Rep* 7:617–621.
35. Koenderman L, van der Linden JA, Honing H, Ulfman LH (2010) Integrins on neutrophils are dispensable for migration into three-dimensional fibrin gels. *Thromb Haemost* 104:599–608.
36. Jannat RA, Robbins GP, Ricart BG, Dembo M, Hammer DA (2010) Neutrophil adhesion and chemotaxis depend on substrate mechanics. *J Phys Condens Matter* 22:194117.